



## Ordered mesoporous carbon coating on cordierite: Synthesis and application as an efficient adsorbent

Ying Wan<sup>a,b,\*</sup>, Xiangting Cui<sup>b</sup>, Zhentao Wen<sup>b</sup>

<sup>a</sup> Key Laboratory of Resource Chemistry of Ministry of Education, Shanghai Key Laboratory of Rare Earth Functional Materials, Shanghai Normal University, Shanghai 200234, P.R. China

<sup>b</sup> Department of Chemistry, Shanghai Normal University, Shanghai 200234, P.R. China

### ARTICLE INFO

#### Article history:

Received 21 May 2011

Received in revised form 8 October 2011

Accepted 10 October 2011

Available online 15 October 2011

#### Keywords:

Honeycomb

Mesoporous carbon

Synthesis

Large processing volume

### ABSTRACT

Ordered mesoporous carbon coating on the honeycomb cordierite substrate has been prepared using low-polymerized phenolic resins as carbon sources and triblock copolymer F127 as the structure directing agent via the evaporation induced self-assembly route. The high-resolution scanning electron microscopy (HRSEM), transmission electron microscopy (TEM), and nitrogen sorption techniques prove the hexagonally ordered pore arrays of carbon coating on the cordierite. The honeycomb monolith adsorbents coated by ordered mesoporous carbons are directly used without any activation, and exhibit adsorption capacities for chlorinated organic pollutants in water with 200 mg/g for *p*-chlorophenol and 178 mg/g for *p*-chloroaniline (with respect to the net carbon coating), high adsorption ratio for low-concentration pollutants, large processing volumes and reusability. More than 200 repeated times can be achieved without obvious loss in both adsorption capacity and weight.

© 2011 Elsevier B.V. All rights reserved.

### 1. Introduction

To remove priority contaminants such as chlorinated organic pollutants in water, various treatments have been investigated, including adsorption [1,2], photodegradation [3], catalytic hydrodechlorination [4], oxidation [5], etc. Among them, adsorption on porous carbons (mainly activated carbons, carbon blacks and activated carbon fibers) is one of the most efficient processes, because of large specific surface areas, pore volumes, chemical inertness and good mechanical stability of carbon [6]. However, the practical applications of these porous carbons are restricted due to the presence of a large amount of micropores, difference in properties from batch to batch, and difficulty in recovery [7]. For adsorption and catalytic reactions, mesopore in the range 5–15 nm is a desired compromise between surface area and accessibility [8]. A post-activation using  $ZnCl_2$ ,  $H_3PO_4$ , or  $H_2O$  is always adopted to expand the pores in activated carbons. After activation, the pore size distribution is wide, that restricts the establishment of the relationship between the pore texture and adsorption properties [9,10]. The additional activation step also produces lots of waste substances and the pore expansion is at the expense of weight loss of carbon, that makes the process uneconomic and environmentally unfriendly. The surface chemistry of activated carbons, in particular from different sources and treatments, is uncertain [11]. Because

the adsorption capacity of a given carbon strongly depends on the chemical nature of the surface [7], the adsorption performance for the same organic pollutant on activated carbon differs from each other. The adsorption behavior cannot be identically compared. The difficult separation of fine carbon powders in water is the major problem in recovery. The loss of carbon results in both uneconomic operation and pollution in water. At the same time, the processing volume is limited [7]. Therefore, porous carbons with uniform pores which can be easily separated and have large processing ability are highly desired for adsorption of poisoning pollutants from water.

Ordered mesoporous carbons possess unique structures, high surface areas and uniform, large and tunable pore channels, showing advantages in adsorption, separation, catalysis, and electrodes. The mesoporous carbon is normally fabricated by nanocasting [12]. Mesoporous silica is chosen as a hard template. Then the carbon source is filled inside the mesopores. Upon carbonization and subsequent removal of the silica scaffold by HF or NaOH solution, ordered mesoporous carbon is produced. This kind of carbon replicas (in most cases, powdered carbons) can be used to adsorb dyes and biomolecules [13]. Among them, magnetically separable ordered mesoporous carbons are attractive because of the recovery of powders by an external magnetic field [14,15]. For example, Schueth and co-workers synthesized magnetically separable ordered mesoporous carbon by introducing magnetic functional species into the porous carbon during nanocasting [15]. Magnetic nanoparticles are selectively deposited on the outer surface of the carbon. After dye adsorption, mesoporous carbon powders can be separated from solution by a magnet. Very recently,

\* Corresponding author. Tel.: +86 21 6432 2516; fax: +86 21 6432 2511.  
E-mail address: [ywan@shnu.edu.cn](mailto:ywan@shnu.edu.cn) (Y. Wan).

the direct synthesis method for ordered mesoporous carbons from the self-assembly of amphiphilic block copolymers and phenolic resins have been reported [16,17]. The carbon materials are directly carbonized from organic polymers, and the ordered pore arrays are originated from self-assembling PPO domains of triblock copolymer. Accordingly, the carbon surface chemistry, pore texture and morphology can be well controlled. For example, Zhao and co-workers used all commercially available, low-cost raw materials, namely phenol, formaldehyde and triblock copolymer, to prepare ordered mesoporous carbon powders with different pore sizes [16]. Liang and Dai prepared carbon fibers with well-aligned mesopores from the phloroglucinol/formaldehyde/Pluronic F127 complex [17]. Flexible carbon sheets can be further woven by the fibers. This simple operation omits the use of hard template, and facilitates the large-scale production of ordered mesoporous carbons and their practical applications in adsorption and catalysis [9,18]. Magnetically separable ordered mesoporous carbon composites have also been prepared by self-assembly of phenol, formaldehyde,  $\text{Fe}(\text{NO}_3)_3 \cdot 9\text{H}_2\text{O}$  and triblock copolymer F127, and used as reusable carbon powders for adsorption [19].

Adsorbent and catalyst coating on inorganic ceramics monoliths are of great significance for industry because of their favorable properties such as low pressure drop, high geometric surface area, short diffusion lengths, lack of attrition by vibration, thermal shock resistance, and convenient separation from media without assistance of outer magnetic field [8,20,21]. Carbon layer can be coated on cordierite monolith by dipcoating with Novalac resin, Furan resin, polyfurfuryl alcohol, etc. Several steps are necessary: dipping the ceramic monolith in the carbon precursor, flushing with pressurized air, a treatment at elevated temperature for curing, carbonization, and activation. The carbon coatings from polyfurfuryl alcohol have always micropores and the mesopores ratios are below 10% [8]. The post-activation under an oxidative condition such as  $\text{CO}_2$  or  $\text{O}_2$  atmosphere is subjected to enhance mesoporosity. However, carbon simultaneously burns off; for example, 30% carbon losses in  $\text{CO}_2$  atmosphere at  $920^\circ\text{C}$  within 4 h [20]. In addition, the pore size distribution is rather wide. Using carbon xerogel as a precursor for carbon layer coating on cordierite foams can increase mesopores of carbon; but reduces the adhesion between ceramic foams and carbon coatings [22]. The coating of ordered mesoporous materials on cordierite with an unsmooth surface has not been reported, but will for certain extend the applications of mesoporous materials especially as adsorbents and catalysts. Here we report the surfactant self-assembly of ordered mesoporous carbon coating on honeycomb cordierite and its application as an adsorbent. Carbon with opened, hexagonally ordered pore arrays can be coated on cordierite with unsmooth surface. Without any further treatment, ordered mesoporous carbon coating on honeycomb cordierite is directly used as a reusable adsorbent. The adsorbent exhibits adsorption ability for *p*-chlorophenol or *p*-chloroaniline, a large processing volume, and great advantage in reusability. Over 200 repeated times adsorption/desorption with negligible losses in both weight and adsorption ability can be achieved. The synthesis of honeycomb monolithic mesoporous carbon involves all commercially available raw materials, as well as is easy, reproducible, and expected to be extended to other mesoporous carbon-based catalysts and adsorbents. These features favor practical applications in industry.

## 2. Materials and methods

### 2.1. Materials

Poly(ethylene oxide)-block-poly(propylene oxide)-block-poly(ethylene oxide) triblock copolymer F127

(PEO<sub>106</sub>PPO<sub>70</sub>PEO<sub>106</sub>,  $M_w = 12,600$ ) was purchased from Acros Chemical Inc. Phenol ( $\text{C}_6\text{H}_5\text{OH}$ , 99.98%), formalin ( $\text{HCHO}$ , 37.0–40.0%), tetraethyl orthosilicate (TEOS,  $\text{SiO}_2 > 28.4\%$ ), hydrogen chloride ( $\text{HCl}$ , 36.0–38.0%), sodium hydroxide ( $\text{NaOH}$ , minimum 96.0%), ethanol ( $\text{C}_2\text{H}_5\text{OH}$ , minimum 99.7%), *p*-chlorophenol ( $\text{Cl}-\text{C}_6\text{H}_4-\text{OH}$ , 99%) and *p*-chloroaniline ( $\text{Cl}-\text{C}_6\text{H}_4-\text{NH}_2$ , 99%) were obtained from Shanghai Chemical Co. Cordierite was purchased from Huayin Ceramic Electromechanical Sci. Tech. Co. Activated carbon was supplied by Shanghai Xinzhuang Activated Carbon Co. All chemicals were used as received without any further purification. Water used in all syntheses was distilled and deionized.

### 2.2. Preparation of ordered mesoporous carbon coating on honeycomb cordierite

Ordered mesoporous carbon coating on honeycomb cordierites were prepared by using the surfactant-templating method with cordierite as a carrier, phenol and formaldehyde as carbon sources and triblock copolymer F127 as a structure-directing agent. Phenol and formaldehyde were firstly polymerized to water- and ethanol-soluble phenolic resins under basic conditions (see details in Supporting Information, SI) [16]. The synthesis procedure for the monolithic mesoporous carbons was carried out as following. Firstly, 4.0 g of triblock copolymer F127 was dissolved in 4.0 g of ethanol to obtain a clear solution. To it, added the mixture with 4.85 g of preformed phenolic resins (containing 2.93 g of phenol and 1.92 g of formaldehyde) and 2.42 g of ethanol. After stirring for 10 min, the mixture was impregnated with cordierite pieces (here, we cut the cordierite into several pieces with the size of  $11\text{ mm} \times 11\text{ mm} \times 38\text{ mm}$ ). To ensure the homogenous coating of carbons precursors, air-flow with a rate of 50 mL/min was used to sweep along the pores of cordierites. Then, the cordierites supported with carbon precursors were placed in a hood to evaporate ethanol at ambient temperature for 5–8 h, in an oven to thermopolymerize at  $100^\circ\text{C}$  for 24 h, and then in a tube furnace which was protected by nitrogen to remove surfactant at  $350^\circ\text{C}$  for 5 h and to carbonize at  $900^\circ\text{C}$  for 4 h. The color of cordierite changed from initially white to black. Before use, honeycomb monolith adsorbents with mesoporous carbon coating were treated in ethanol under ultrasonic (200 W, 50 Hz) with 5 min.

Activated carbon coating on honeycomb cordierite was prepared according to the above procedure without the use of triblock copolymer.

For comparison, mesoporous carbon films on silicon wafer were prepared by using silicon wafer as a substrate to replace cordierite. The mixture containing low-polymerized phenolic resins, triblock copolymer F127 and ethanol were deposited on silicon wafer by spin-coating. All other steps are exactly the same as described above. When the precursor solution contains 4.0 g of triblock copolymer F127, 2.5 g of preformed phenolic resins, 5.2 g of TEOS, 2.5 g of  $\text{HCl}$  (0.2 M), and 5.3 g of ethanol, mesoporous carbon-silica films on silicon wafer were also prepared [23]. In a separated synthesis, glass disks were used as the substrate to coat mesoporous carbon. After thermopolymerized at  $100^\circ\text{C}$ , the bakelite/triblock copolymer composites were scraped from the glass substrate and grinded into powders, and carbonized as described above. This sample was denoted as pristine powdered mesoporous carbon.

### 2.3. Characterization

The small-angle X-ray diffraction (XRD) measurements were taken on a Rigaku D/max B diffractometer using  $\text{Cu K}\alpha$  radiation (40 kV, 20 mA). The *d*-spacing values were calculated by the formula of  $d = 0.15408 / 2 \sin \theta$ , and the unit-cell parameters were calculated from the formula of  $a_0 = 2d_{10}\sqrt{3}$ .  $\text{N}_2$  adsorption-desorption isotherms were measured at 77 K with Quantachrome NOVA 4000e

analyzer. The Brunauer–Emmett–Teller (BET) method was utilized to calculate the specific surface areas ( $S_{\text{BET}}$ ). By using the Barrett–Joyner–Halenda (BJH) model, the pore volumes and pore size distributions were derived from the adsorption branches of isotherms, and the total pore volumes ( $V_{\text{t}}$ ) were estimated from the adsorbed amount at a relative pressure  $p/p_0$  of 0.99. The micropore volume ( $V_{\text{micro}}$ ) and micropore surface area were calculated from the  $V-t$  plot method. The  $t$  values were calculated as a function of the relative pressure using the de Boer equation,  $t/\text{Å} = [13.99/(\log(p_0/p) + 0.0340)]^{1/2}$ .  $V_{\text{micro}}$  was obtained using the equation  $V_{\text{micro}}/\text{cm}^3 = 0.001547I$ , where  $I$  represents the Y intercept in the  $V-t$  plot. The sample morphology was observed with a high-resolution scanning electron microscopy (HRSEM, Hitachi S 5500). Transmission electron microscopy (TEM) experiments were conducted using a JEOL 2011 microscope operated at 200 kV. The samples for TEM measurements were suspended in ethanol and supported onto a holey carbon film on a Cu grid. Weight losses and the associated temperatures were determined by thermogravimetry analysis with a Mettler Toledo TG/SDTA 851e apparatus. Samples were heated from room temperature to 1000 °C at a rate of 10 °C/min in air flow.

#### 2.4. Batch mode adsorption

The batch mode adsorption studies for various chlorinated organic pollutants, such as *p*-chlorophenol and *p*-chloroaniline, were carried out by agitating 1.6 g of honeycomb adsorbent (11 mm × 11 mm × 38 mm) supported with mesoporous carbon (0.07–0.23 g) in 50 mL of mixture (water and chlorinated organic pollutant). The mixture containing 50 mL of water and a certain amount of *p*-chlorophenol (0.031–0.312 mmol) or *p*-chloroaniline (0.041–0.314 mmol) was continuously shaken in a shaking bath with a speed of 120 rpm at 30 °C until the equilibrium was reached (typically 24 h). After adsorption, the honeycomb monolithic mesoporous carbon adsorbent was taken out for further regeneration. The concentration of *p*-chlorophenol or *p*-chloroaniline in the residue liquid mixture was determined using a XinMao Ultraviolet–visible (UV–vis) spectrophotometer (UV-7504 PC). The adsorption tests and each concentration analysis were repeated at least three times, and the experimental errors were within ±5%. For comparison, powdered mesoporous carbon and activated carbons with the same carbon weight were also tested as an adsorbent. The mixture was centrifuged at 4000 rpm for 5 min after adsorption. The pollutant concentration in the supernatant was determined as mentioned above.

The equilibrium adsorption capacities ( $Q_e$ ) were determined according to the following formula:  $Q_e = (C_i - C_e) \times V/m$ , wherein  $C_i$  is the initial concentration,  $C_e$  is the residual or equilibrium concentration,  $V$  is the volume of the liquid phase,  $m$  is the mass of the adsorbent. The saturated adsorption loading  $Q_0$  was calculated from the linearized Langmuir equation:  $C_e/Q_e = 1/Q_0b + C_e/Q_0$ .

#### 2.5. Quality control and quality assurance

Standard solutions were analyzed every 8 sample solutions as a check on the instrument performance of the UV–vis spectrophotometer. The precision of each sample was determined in duplicate, and only values below 5% were accepted, with other samples outside this range being reanalyzed.

All the adsorption experiments were repeated three times and average values were reported. The standard deviation was found to be ±3%. The measurements were within the uncertainty margins of the reference materials, thus demonstrating the accuracy of our findings.

#### 2.6. Regeneration of adsorbent material

The procedure for regeneration was as follows [24]. The chosen regenerant (20 mL of ethanol) was added to the vessel were treated with ultrasonic (200 W, 50 Hz) for 5 min. The regenerant was then separated and analyzed spectrophotometrically for desorbed *p*-chlorophenol. After the treatment (with regenerants), 25 mL of distilled water was used to rinse the material. Any amount of *p*-chlorophenol removed by water was not considered for regeneration efficiency (RE) calculations. Regenerated monolithic mesoporous carbons were dried and subsequently placed in contact with a fresh solution of the adsorbate for the second adsorption with all test conditions retaining the same. After adsorption, the honeycomb monolithic mesoporous carbon adsorbent was taken out for further regeneration. The residue liquid was analyzed and the uptake of substituted phenols was calculated. The spent carbon was again regenerated and exhausted for 200 cycles.

### 3. Results and discussion

The mesoporous carbon was deposited on cordierite by coating the ethanol solution of preformed phenolic resins and triblock copolymer template. The synthesis involves all commercial raw materials and the process is simple. The as-made materials are uniform light-brown films coated on cordierite without cracking (Fig. S1). After carbonization at 900 °C, the honeycomb monolithic adsorbents become black indicating the transformation from polymer to carbon. Optical photos for a blank cordierite, and the so-derived monolithic carbon adsorbent with the size of 11 mm × 11 mm × 38 mm are shown in Fig. 1. The honeycomb monoliths with carbon coating show no change in macroscopic size upon carbonization on comparison with the blank cordierite carrier. The weight ratios of carbon are about 4.4 wt%, measured by the TG analysis. Negligible weight losses are detected after repeatedly shaking the monolithic mesoporous carbon @ cordierite adsorbents in ethanol solution under ultrasonic (200 W, 50 Hz) for 100 times and each time for 5 min. Each time the monolithic adsorbents are taken out, dried at 100 °C, and then put in the same ethanol solution. No black carbon powders can be found after evaporation of the final ethanol solution. These results indicate the stability of mesoporous carbon coatings.

HRSEM images for ordered mesoporous carbon coating on honeycomb cordierite after carbonization show relatively uniform surface, with crystals in some domains (Fig. 1d). Well aligned uniform pores can be observed in the image with a high magnification (Fig. 1f), indicating the ordered mesostructure of coating after carbonization. The film thickness is about 9 μm which is visually measured in the HRSEM image of the cross-section (Fig. 1e). To further investigate the pore properties of mesoporous carbon adsorbent by TEM and nitrogen sorption techniques, the coatings were scraped from inorganic substrate (the scraped powders contain both carbon coating and inorganic cordierite in this case). TEM images for mesoporous carbons scraped from cordierite reveal the hexagonally arranged and stripe-like pores (Fig. 1g and h), suggesting that the mesoporous carbon coating has the 2D hexagonal mesostructure.  $N_2$  sorption isotherms show that the scraped mesoporous carbon (in a weight ratio of 78 wt% of carbon determined by the TG analysis) has representative type-IV curves with an H2-type hysteresis loop (Fig. 2), indicative of the presence of opened, ordered mesopores. Because the inorganic cordierite has no nanosized pores and possesses an extremely low surface area, the nitrogen adsorption in the middle relative pressures is caused by the mesoporous carbon coating. The surface area for the ordered mesoporous carbon coating is 494 m<sup>2</sup>/g, the pore volume is 0.40 cm<sup>3</sup>/g and the most possible mesopore size is 3.9 nm. The  $V-t$

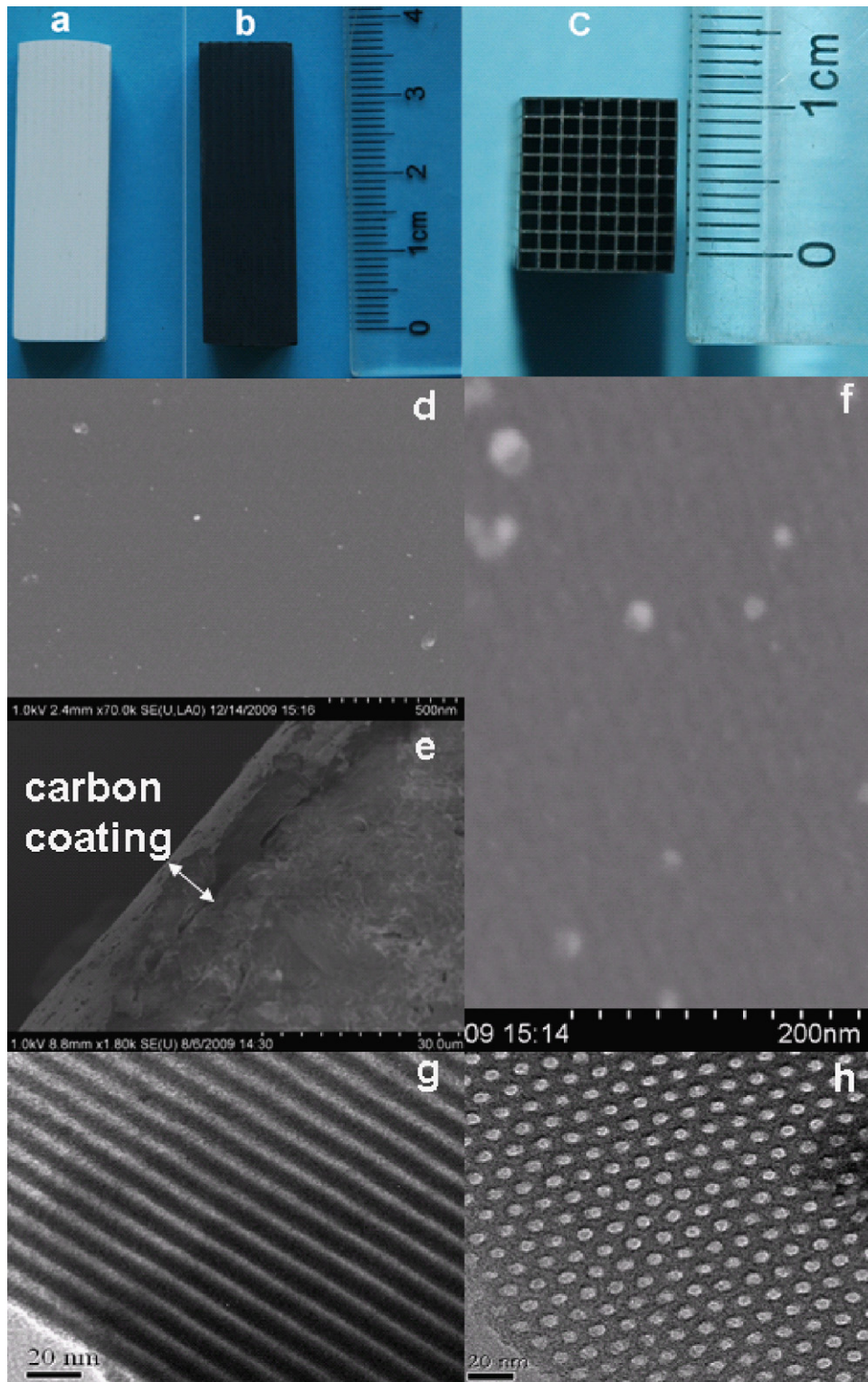


**Fig. 1.** (a–c) Optical photos and (d–f) HRSEM images for (a) blank cordierite, and (b–f) cordierite after coating with ordered mesoporous carbon: (a and b) side view, (c) top view, (d) top view, (e) top view with a high magnification, and (f) cross-section. (g and h) TEM images for mesoporous carbons scraped from cordierite viewed (g) perpendicular and (h) parallel to the pore channels.

plot analysis reveals micropore volume of  $0.10 \text{ cm}^3/\text{g}$ , suggesting that the mesopore volume of the carbon coating contributes 75% to the total volume (Fig. S2). The pore properties are analogous to those for ordered mesoporous carbon powders reported by Zhao and co-workers [16], indicating that coating on cordierite shows a minor effect on the textural properties of the mesoporous carbon.

The XRD pattern of the as-made bakelite/F127 composite coating on cordierite shows a strong diffraction peak at  $2\theta$  of  $0.68^\circ$ , indicative of the ordered mesostructure (Fig. 3). However, no distinct diffraction can be observed after carbonization. This phenomenon is in disagreement with the HRSEM and TEM results which show large-domain ordered mesopore arrays, and quite different with

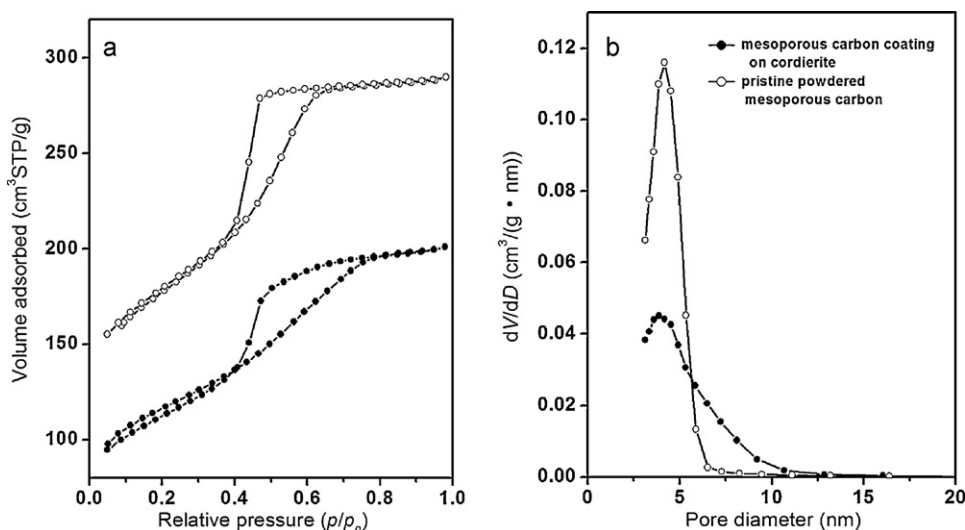


**Fig. 2.** (a)  $N_2$  sorption isotherms and (b) pore-size distribution curves of mesoporous carbon coating on the honeycomb cordierite. The curves are measured on mesoporous carbon which is scraped from the cordierite monolith. The carbon content in scraped powders is 78 wt% measured by the TG analysis. For comparison, pristine powdered mesoporous carbon is also tested.

pristine powdered ordered mesoporous carbon [16]. Well resolved diffraction peaks can be clearly seen in the small-angle XRD patterns for the latter materials both before and after carbonization.

In order to understand the formation of mesoporous carbon coating on cordierite, carbon was also coated on the silicon wafer or glass disk substrate using the same synthesis compositions. If the as-made bakelite/F127 composite coating is directly scraped from the silicon wafer or glass disk and grinded, the as-made pristine powdered material shows the ordered mesostructure, as evidenced by the well-resolved XRD pattern (Fig. 3). After carbonization at 900 °C, the powdered carbon displays three diffraction peaks, assignable to the highly ordered 2D hexagonal mesostructure. The framework shrinkage is about 32% after carbonization. The powdered carbon exhibits a BET surface area of 582 m<sup>2</sup>/g, a pore volume

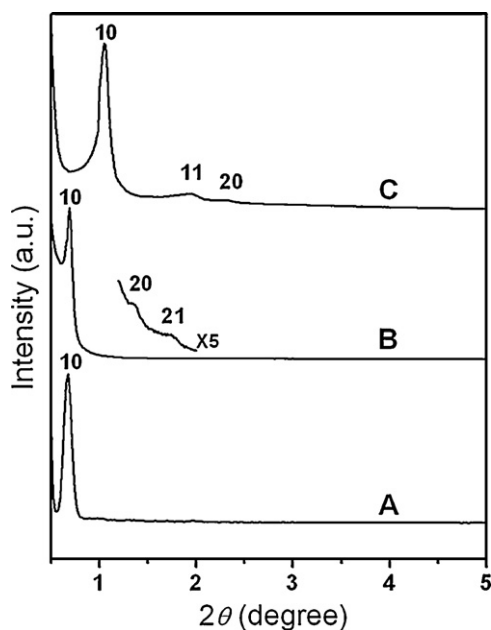


**Fig. 3.** XRD patterns of (A) as-made bakelite/F127 composite coating on honeycomb cordierite; (B) as-made pristine powdered bakelite/F127 composite which is scraped from glass disk substrate; (C) the powdered sample (B) after carbonization at 900 °C under nitrogen.

of 0.45 cm<sup>3</sup>/g, and a quite uniform mesopore size centred at 4.2 nm (Fig. 2). These results are in good agreement with the literature [16]. However, no ordered materials can be obtained if carbonization at 900 °C is directly taken for the as-made bakelite/F127 composite coating on silicon wafer. The HRSEM and TEM images cannot find ordered pore arrays. This result is different with either the mesoporous carbon film on cordierite or the mesoporous silica film on silicon wafer. Ordered mesoporous silica films can be well coated on silicon wafer after calcination [25]. In fact, compact and smooth surfaces, including mica [26], interface of water and air [27], glass, and polymer [28] films have also been used to support ordered mesoporous silica films.

The possible reason for the different phenomena of mesoporous carbon and silica films on smooth silicon wafer lies in the fact that these two materials have distinct difference in framework shrinkage upon calcination. The mesoporous carbon shows a large framework shrinkage after carbonization at 900 °C (about 30–40%), because of the cross-linkage of phenolic resins and the release of small molecules [16]. Once the carbon precursor (phenolic resol) is coated on a smooth surface (such as silicon wafer), the framework shrinkage upon carbonization and the reservation of the macroscopic size due to the interface interaction between surface and carbon, play opposite roles, destroying the mesostructure. Therefore, no ordered mesoporous carbon films can be obtained on the smooth silicon wafer surface. By comparison, the framework shrinkage for silica is small (about 10% for the SBA-15 mesoporous silica) [29]. The mesostructured silica thin films on silicon wafer can be preserved upon calcination. Following this idea, we add silica nanoparticles inside the mesoporous carbon framework which can distinctly reduce the framework shrinkage [23]. As expected, the ordered mesopore arrays can be found in large areas for the mesoporous carbon–silica thin films coated on silicon wafer (Fig. S3).

Therefore, the formation of ordered mesoporous carbon coatings on cordierite may be attributed to the unsmooth surface (Fig. 4). Inorganic cordierite is directly used without any further treatment. The HRSEM image for cordierite depicts a dense microstructure with crystals of granular habit (Fig. S4). The surface of cordierite is unsmooth, as well as plenty of and continuous voids are presented between granular crystals. The voids can be occupied by the bakelite/F127/ethanol solution. The tiny pieces of granular crystals in cordierite serve as substrates for the carbonaceous coating. Upon carbonization at 900 °C, the mesostructure destruction

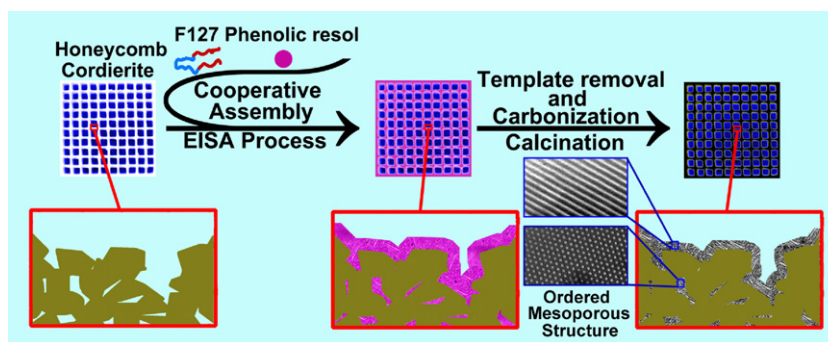


Fig. 4. Scheme for the formation of ordered mesoporous carbon coatings on unsmooth surface of cordierite.

which is caused by the competition of the large framework shrinkage of carbon and interface interaction can be avoided to some extent due to the strain field by the tiny substrate. On the other hand, the mesoporous carbon precursors inside voids may act as cross-linking sites. Ordered mesoporous carbon films can be eventually formed both on the surface and in the voids because of local carbonization. As mentioned above, no distinct diffraction peak can be observed in the small-angle XRD pattern for the mesoporous carbon coating on honeycomb cordierite after carbonization, possibly due to the unsmooth and discontinuous surface of cordierite and the EISA process. The tiny pieces of granular crystals in cordierite serve as the substrate for carbon coating. The unsmooth surface of cordierite, in particular some raised tiny pieces of granular crystals is distinctly exposed after carbonization of bakelite, as shown in Fig. 1d. The discontinuous carbon film is one of the major reasons for the lack of diffraction peaks. Secondly, the samples prepared by the EISA method normally require certain substrates for controlled deposition, which imposes a strain field, generating a uniaxial lattice distortion. This distortion lowers the mesostructure symmetry [30,31].

The honeycomb cordierite adsorbents with mesoporous carbon coating are directly utilized to remove chlorinated organic pollutants in water without any further activation. In a batch containing *p*-chlorophenol or *p*-chloroaniline, water, and/or blank cordierite, negligible concentration change can be observed for organic compounds after shaking for 24 h. Only when the honeycomb monolithic adsorbent with carbon coating is added to the batch (one piece of honeycomb coated by mesoporous carbon adsorbent is mixed with 50 mL of polluted water), distinct variation can be detected, indicative of adsorption by carbon coating and the accessibility of pores in the coating. The equilibrium adsorption isotherms for *p*-chlorophenol and *p*-chloroaniline belong to type-I curve, characteristic Langmuir (Fig. 5). The amount of adsorbed *p*-chlorophenol and *p*-chloroaniline dramatically increase at a low final solution concentration, suggesting a high affinity between the chlorine-containing organic molecule and the carbonaceous adsorbent surface [29,30], and the adsorbed amount reaches a plateau at a high equilibrium solution concentration, reflecting the saturated adsorption. Honeycomb monolith with mesoporous carbon coating exhibits an adsorption capacity of 200 mg/g for *p*-chlorophenol and 178 mg/g for *p*-chloroaniline with respect to the net carbon coating. The sorption capacities are comparably to those on adsorbents reported in literatures most of which requires a further activation step (Tables S1 and S2). The large adsorption ability is possibly due to the large pore volume, high surface area of mesoporous carbon, and the attraction between the  $\pi$  orbital on the carbon basal planes and the electronic density in the aromatic rings ( $\pi$ - $\pi$  interactions).

On consideration of the specific surface area for the adsorbent and molecular dimensions for adsorbates, the surface coverage over mesoporous carbon coating is large (0.915 for *p*-chlorophenol

and 0.831 for *p*-chloroaniline). The slight difference in the adsorption ability of *p*-chlorophenol and *p*-chloroaniline by monolithic mesoporous carbon is thus possibly related to solubility in water and polarity of organic substances. Several groups have found the adsorption amount of different substrates varies each other over carbon-based adsorbent such as carbon nanotubes with high surface areas and a certain functional groups, and attempted to correlate the adsorption ability between the adsorbent and adsorbate [32]. However, no apparent trends of linearity can be generalized on the basis of either chemical properties (e.g., polarity, hydrophobicity, or size of the adsorbates) or properties of the carbon nanotubes (e.g., single-walled vs multiwalled carbon tubes, or wall diameter of the carbon nanotubes). Since the studied carbon adsorbent is derived from carbonization of resins, the surface functional groups may show affinity to organic substances. A detailed study of the adsorption ability for organic pollutants with different polarity, electronic polarity, solubility, etc. over monolithic mesoporous carbon is deserved to develop and separately reported.

When the processing volume is increased to 1L, 20 pieces of honeycomb monolithic mesoporous carbon are used to adsorb *p*-chlorophenol from water. A similar adsorption property is obtained (205 mg/g based on the carbon coating). After adsorption, the honeycomb adsorbents are taken out from water, and put into ethanol solution under ultrasonic. A 97% desorption of *p*-chlorophenol and negligible weight loss can be achieved. The recovered adsorbents are then used to adsorb organic pollutant again, displaying the similar adsorption ability with the fresh ones. Over 200 repeated

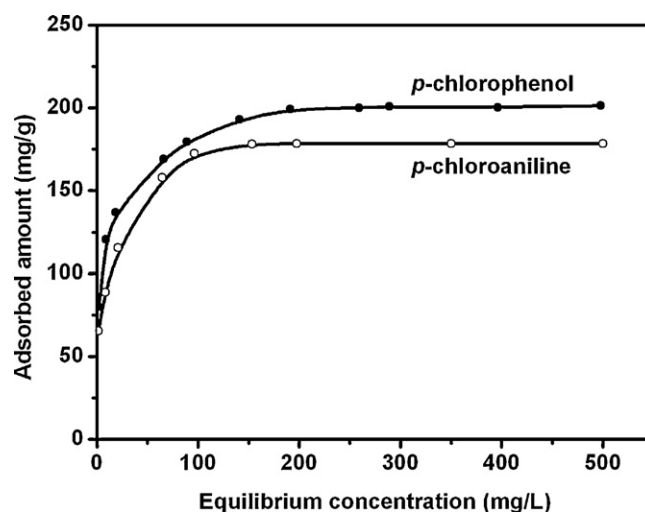


Fig. 5. Adsorption isotherms for *p*-chlorophenol and *p*-chloroaniline on honeycomb adsorbent with ordered mesoporous carbon coating. The adsorption ability is calculated on the basis of the carbon coating.

**Table 1**  
Saturated adsorption amount of *p*-chlorophenol on the honeycomb adsorbent with different ordered mesoporous carbon loading.

Coating times	Carbon coating weight (g)	Carbon coating weight percentage (wt%)	Adsorption amount (mg/g)		
			With respect to honeycomb adsorbent	With respect to carbon coating	With respect to the adjacent two carbon coating layers
1	0.070	4.4	8.8	200	200
2	0.110	6.7	12.9	191	191
3	0.150	9.0	8.5	95	178
4	0.178	10.5	7.1	68	178
5	0.198	11.5	5.9	51	210
6	0.215	12.4	4.7	38	221
7	0.230	13.1	3.9	30	215

adsorption/desorption were tested. The regeneration efficiency in the first 10 cycles is above 93%. When the repeated times reaches 10, the regeneration efficiency is above 99%. This indicate almost complete recovery of the adsorbents by ethanol under ultrasonic. Negligible adsorption amount loss for the honeycomb adsorbents after 200 times adsorption/desorption cycles (Fig. 6). In addition, weight loss for ordered mesoporous carbon coating on cordierites is undetectable. These results further indicate that the mesoporous carbon coating is stable (the loss of carbon can be avoided during adsorption and elution), and can be easily recovered, showing great potential for applications in industry. Activated carbon layer can be coated on cordierite monolith with Novalac resin, Furan resin, polyfurfuryl alcohol, carbon xerogels, etc. [8,20–22]. Here we used low-polymerized phenolic resins as precursors to coat carbon on honeycomb cordierite. After one-time coating, the carbon coating weight ratio is about 5.9 wt% in the monolith. N<sub>2</sub> physisorption analysis reveals that the carbon coating has a low BET surface area of 22 m<sup>2</sup>/g, similar to the polyfurfuryl alcohol coating on cordierite [21], indicative of small micropores or pore constrictions at the entrance of the micropores, making the microporosity almost inaccessible to the N<sub>2</sub> molecules at –196 °C. This sample shows an adsorption ability to *p*-chlorophenol of 16 mg/g, much lower than mesoporous carbon coating on cordierite which has a high BET surface area, large pore volume, uniform mesopore size and high mesoporosity. Therefore, the presence of triblock copolymer in the synthesis batch is essential for the direct generation of mesopores and interpenetrated micropores in the mesoporous carbon coating on cordierite. And the large amount of accessible pores is responsible for the high adsorption performance. To improve mesoporosity and the adsorption ability of activated carbon coating on cordierite monolith, the post-oxidation for activation is necessary, which has been sufficiently reported [8,20–22]. The etching of pores during

activation is accompanied with the burn-off of carbon. About 25–30% carbon losses [20]. By comparison, the current synthesis for mesoporous carbon coating on cordierite is more simple, convenient and economic than the reported coating of carbon layers from resins or xerogels [8], which omits the activation step.

The adsorption ability to a low concentration is extremely important, because this value is a decisive factor for the residue concentration of organic pollutants in water. The ordered mesoporous carbon coating on cordierite shows a high adsorption ability for polluted water with the concentration of *p*-chlorophenol of 30 mg/L. Negligible chlorinated organic contaminant can be detected after 24-h adsorption.

The loading amount of mesoporous carbon on honeycomb cordierite can be further increased by multiple coating with preformed phenolic resins/F127 mixture. For example, the mesoporous carbon coating weight ratio in honeycomb adsorbent can increase to 12.1 wt% after coating by seven times. The carbon coatings are stable under ultrasonic washing conditions. However, the adsorption amount of *p*-chlorophenol on account of the honeycomb adsorbent undergoes an increase with the increase of carbon coating weight to 6.7 wt% (two-times coating, Table 1), and then a steady reduce with a further increase in carbon weight percentage. Even if the contacting time is prolonged to 72 h, the adsorption amount of *p*-chlorophenol remains almost the same over the honeycomb adsorbents. When the adsorption amount is calculated with respect to the adjacent two carbon layers, the value keeps almost unchanged. The results imply that the initial carbon coatings cannot be fully accessed by organic molecules when the carbon coatings are over-thick. Only two adjacent coating layers on the surface are accessible. The feature may be related with the carbon material, which covers the surface, and inhibits the mass transfer.

#### 4. Conclusion

In summary, honeycomb monolithic ordered mesoporous carbons have been prepared from the surfactant-templating approach using phenol and formaldehyde as carbon sources, triblock copolymer F127 as a structure-directing agent and inorganic cordierite as a substrate; and directly used as reusable adsorbents without any further activation. The honeycomb cordierite based mesoporous carbon coatings have the well-aligned mesopore arrays with the most possible sizes of about 4.0 nm, BET surface areas of about 500 m<sup>2</sup>/g, pore volumes of about 0.40 cm<sup>3</sup>/g, adsorption amounts of 200 mg/g for *p*-chlorophenol (with respect to the net carbon coating) and of 178 mg/g for *p*-chloroaniline, high adsorption ratio for low-concentration pollutants, large processing volumes and reusability. More than 200 times adsorption/desorption can be repeated without obvious losses in both weight and adsorption ability. This method is expected to be extended to other monolithic mesoporous carbon-based catalysts and adsorbents.

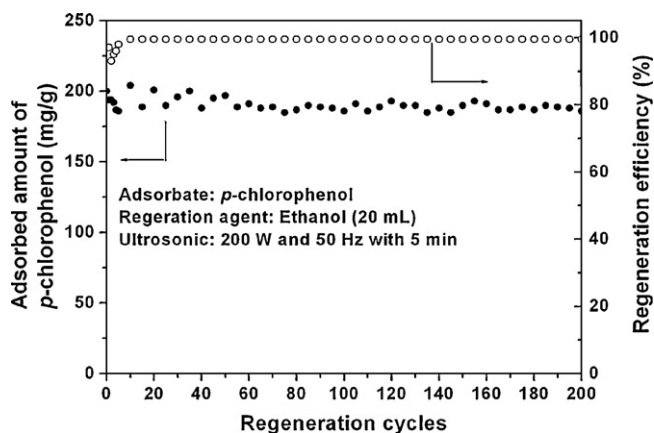


**Fig. 6.** Repeated adsorption test on the honeycomb monolithic adsorbent with ordered mesoporous carbon coating. The adsorption ability is calculated on the basis of the net carbon coating.

## Supporting information

Synthesis procedure of carbon precursors; saturated capacity,  $Q_0$  (mg/g and mg/m<sup>2</sup>) and surface coverage,  $\theta$  for adsorption of *p*-chlorophenol and *p*-chloroaniline by various adsorbents; HRSEM images of as-made bakelite/F127 composite coated on cordierite, carbonized ordered mesoporous silica–carbon film coated on silicon wafer, and blank cordierite;  $V-t$  plot analysis for mesoporous coatings scraped from honeycomb cordierite and pristine powdered mesoporous carbon.

## Acknowledgments

This work was supported by NSF of China (20873086, 21073122 and 21173149), Shanghai Sci. & Tech. and Edu. Committee (10XD1403300, and S30406), the Fok Ying Tung Education Fund (121013). We would like to thank Dr. Y.F. Shi and Prof. D.Y. Zhao for helpful discussion.

## Appendix A. Supplementary data

Supplementary data associated with this article can be found, in the online version, at doi:10.1016/j.jhazmat.2011.10.031.

## References

- [1] M. Ahmaruzzaman, Adsorption of phenolic compounds on low-cost adsorbents: a review, *Adv. Colloid Interface Sci.* 143 (2008) 48–67.
- [2] B. Pavoni, D. Drusian, A. Giacometti, M. Zanette, Assessment of organic chlorinated compound removal from aqueous matrices by adsorption on activated carbon, *Water Res.* 40 (2006) 3571–3579.
- [3] M.M. Cheng, W.H. Ma, C.C. Chen, J.N. Yao, J.C. Zhao, Photocatalytic degradation of organic pollutants catalyzed by layered iron(II) bipyridine complex–clay hybrid under visible irradiation, *Appl. Catal. B* 65 (2006) 217–226.
- [4] A. Elola, E. Diaz, S. Ordonez, A new procedure for the treatment of organochlorinated off-gases combining adsorption and catalytic hydrodechlorination, *Environ. Sci. Technol.* 43 (2009) 1999–2004.
- [5] M. Taralunga, J. Mijoin, P. Magnoux, Catalytic destruction of chlorinated POPs – catalytic oxidation of chlorobenzene over PtHFAU catalysts, *Appl. Catal. B* 60 (2005) 163–171.
- [6] D.Q. Zhu, J.J. Pignatello, Characterization of aromatic compound sorptive interactions with black carbon (charcoal) assisted by graphite as a model, *Environ. Sci. Technol.* 39 (2005) 2033–2041.
- [7] G. Crini, Non-conventional low-cost adsorbents for dye removal: a review, *Bioresour. Technol.* 97 (2006) 1061–1085.
- [8] E. Garcia-Bordeje, F. Kapteijn, J.A. Moulijn, Preparation and characterisation of carbon-coated monoliths for catalyst supports, *Carbon* 40 (2002) 1079–1088.
- [9] X. Zhuang, Y. Wan, C.M. Feng, Y. Shen, D.Y. Zhao, Highly efficient adsorption of bulky dye molecules in wastewater on ordered mesoporous carbons, *Chem. Mater.* 21 (2009) 706–716.
- [10] G.M. Walker, L.R. Weatherley, Adsorption of dyes from aqueous solution – the effect of adsorbent pore size distribution and dye aggregation, *Chem. Eng. J.* 83 (2001) 201–206.
- [11] N. Wibowo, L. Setyadhi, D. Wibowo, J. Setiawan, S. Ismadji, Adsorption of benzene and toluene from aqueous solutions onto activated carbon and its acid and heat treated forms: influence of surface chemistry on adsorption, *J. Hazard. Mater.* 146 (2007) 237–242.
- [12] (a) A.H. Lu, F. Schuth, Nanocasting: a versatile strategy for creating nanostructured porous materials, *Adv. Mater.* 18 (2006) 1793–1805; (b) Y. Wan, H.F. Yang, D.Y. Zhao, “Host–guest” chemistry in the synthesis of ordered nonsiliceous mesoporous materials, *Acc. Chem. Res.* 39 (2006) 423–432.
- [13] A. Vinu, M. Miyahara, K. Ariga, Biomaterial immobilization in nanoporous carbon molecular sieves: influence of solution pH, pore volume, and pore diameter, *J. Phys. Chem. B* 109 (2005) 6436–6441.
- [14] (a) D. Mohan, A. Sarswat, V.K. Singh, M. Alexandre-Franco, C.U. Pittman Jr., Development of magnetic activated carbon from almond shells for trinitrophenol removal from water, *Chem. Eng. J.* 172 (2011) 1111–1125; (b) S. Singh, K.C. Barick, D. Bahadur, Surface engineered magnetic nanoparticles for removal of toxic metal ions and bacterial pathogens, *J. Hazard. Mater.* 192 (2011) 1539–1547.
- [15] A.H. Lu, W. Schmidt, N. Matoussevitch, H. Bonnemann, B. Spliethoff, B. Tesche, E. Bill, W. Kiefer, F. Schuth, Nanoengineering of a magnetically separable hydrogenation catalyst, *Angew. Chem. Int. Ed.* 43 (2004) 4303–4306.
- [16] Y. Meng, D. Gu, F.Q. Zhang, Y.F. Shi, H.F. Yang, Z. Li, C.Z. Yu, B. Tu, D.Y. Zhao, Ordered mesoporous polymers and homologous carbon frameworks: amphiphilic surfactant templating and direct transformation, *Angew. Chem. Int. Ed.* 44 (2005) 7053–7059.
- [17] C.D. Liang, S. Dai, Synthesis of mesoporous carbon materials via enhanced hydrogen-bonding interaction, *J. Am. Chem. Soc.* 128 (2006) 5316–5317.
- [18] Y. Wan, H.Y. Wang, Q.F. Zhao, M. Klingstedt, O. Terasaki, D.Y. Zhao, Ordered mesoporous Pd/silica–carbon as a highly active heterogeneous catalyst for coupling reaction of chlorobenzene in aqueous media, *J. Am. Chem. Soc.* 131 (2009) 4541–4550.
- [19] Y.P. Zhai, Y.Q. Dou, X.X. Liu, B. Tu, D.Y. Zhao, One-pot synthesis of magnetically separable ordered mesoporous carbon, *J. Mater. Chem.* 19 (2009) 3292–3300.
- [20] E. Garcia-Bordeje, M.J. Lazaro, R. Moliner, P.M. Alvarez, V. Gomez-Serrano, J.L.G. Fierro, Vanadium supported on carbon coated honeycomb monoliths for the selective catalytic reduction of NO at low temperatures: influence of the oxidation pre-treatment, *Carbon* 44 (2006) 407–417.
- [21] A.F. Perez-Cadenas, F. Kapteijn, J.A. Moulijn, F.J. Maldonado-Hodar, F. Carrasco-Marin, C. Moreno-Castilla, Pd and Pt catalysts supported on carbon-coated monoliths for low-temperature combustion of xylenes, *Carbon* 44 (2006) 2463–2468.
- [22] F.J. Maldonado-Hodar, S. Morales-Torres, F. Ribeiro, E.R. Silva, A.F. Perez-Cadenas, F. Carrasco-Marin, F.A.C. Oliveira, Development of carbon coatings for cordierite foams: an alternative to cordierite honeycombs, *Langmuir* 24 (2008) 3267–3273.
- [23] R.L. Liu, Y.F. Shi, Y. Wan, Y. Meng, F.Q. Zhang, D. Gu, Z.X. Chen, B. Tu, D.Y. Zhao, Triconstituent Co-assembly to ordered mesostructured polymer–silica and carbon–silica nanocomposites and large-pore mesoporous carbons with high surface areas, *J. Am. Chem. Soc.* 128 (2006) 11652–11662.
- [24] S.K. Srivastava, R. Tyagi, Organic desorption and chemical regeneration of spent carbon developed from fertilizer waste slurry, *J. Environ. Eng.* 121 (1995) 186–193.
- [25] Y.F. Lu, R. Ganguli, C.A. Drewien, M.T. Anderson, C.J. Brinker, W.L. Gong, Y.X. Guo, H. Soyez, B. Dunn, M.H. Huang, J.I. Zink, Continuous formation of supported cubic and hexagonal mesoporous films by sol–gel dip-coating, *Nature* 389 (1997) 364–368.
- [26] H. Yang, A. Kuperman, N. Coombs, S. MamichAfara, G.A. Ozin, Synthesis of oriented films of mesoporous silica on mica, *Nature* 379 (1996) 703–705.
- [27] H. Yang, N. Coombs, I. Sokolov, G.A. Ozin, Free-standing and oriented mesoporous silica films grown at the air–water interface, *Nature* 381 (1996) 589–592.
- [28] T. Suzuki, H. Miyata, K. Kuroda, Phenylene-bridged mesoporous organosilica films with uniaxially aligned mesochannels, *J. Mater. Chem.* 18 (2008) 1239–1244.
- [29] D.Y. Zhao, Q.S. Huo, J.L. Feng, B.F. Chmelka, G.D. Stucky, Nonionic triblock and star diblock copolymer and oligomeric surfactant syntheses of highly ordered, hydrothermally stable, mesoporous silica structures, *J. Am. Chem. Soc.* 120 (1998) 6024–6036.
- [30] D. Grosso, F. Cagnol, G. Soler-Illia, E.L. Crepaldi, H. Amenitsch, A. Brunet-Bruneau, A. Bourgeois, C. Sanchez, Fundamentals of mesostructuring through evaporation-induced self-assembly, *Adv. Funct. Mater.* 14 (2004) 309–322.
- [31] B.Z. Tian, X.Y. Liu, L.A. Solovoyov, Z. Liu, H.F. Yang, Z.D. Zhang, S.H. Xie, F.Q. Zhang, B. Tu, C.Z. Yu, O. Terasaki, D.Y. Zhao, Facile synthesis and characterization of novel mesoporous and mesorelief oxides with gyroidal structures, *J. Am. Chem. Soc.* 126 (2004) 865–875.
- [32] (a) W. Chen, L. Duan, D.Q. Zhu, Adsorption of polar and nonpolar organic chemicals to carbon nanotubes, *Environ. Sci. Technol.* 41 (2007) 8295–8300; (b) K. Yang, L. Zhu, B. Xing, Adsorption of polycyclic aromatic hydrocarbons by carbon nanomaterials, *Environ. Sci. Technol.* 40 (2006) 1855–1861.